

**Lévy walks in random scattering and growth of waves**

P. M. Drysdale\* and P. A. Robinson†

*School of Physics, University of Sydney, Sydney, New South Wales 2006, Australia*

(Received 28 June 2004; published 17 November 2004)

Random spatial wave scattering and stochastic wave growth are studied where one or both of the random processes can be described by a Lévy walk. This analysis extends previous work on randomly growing and scattering waves where both the random processes are modeled by Gaussian diffusive statistics. Both random spatial scattering and stochastic wave growth modeled by Lévy walks are studied separately, together, and in combination with Gaussian processes. Transmission coefficients, lasing thresholds, and energy densities in the medium are obtained for the different permutations.

DOI: 10.1103/PhysRevE.70.056112

PACS number(s): 02.50.-r, 05.40.Fb

**I. INTRODUCTION**

In propagating through a random medium, waves can scatter spatially and/or grow with a randomly varying growth rate. For strongly scattering media such as biological tissue or paint, the propagation may be so strongly randomized that wave scattering can be described by a scalar diffusion equation [1]. Similarly, waves growing with randomly varying growth rates have been used to model waves in space plasmas using stochastic growth theory [2]. Spatial scattering of waves may also occur, combined with either a constant wave growth or a random varying wave growth rate [3,4]. In each of these cases the random processes commonly used to model the random scattering or growth are termed Gaussian or diffusive. In this paper these studies are extended to situations where the spatial diffusion or random growth of the waves, or both, are not Gaussian. Since Gaussian systems are diffusive, the underlying random walk process's mean square displacement increases linearly with time  $\langle r^2 \rangle \sim t$ . In a superdiffusive system the mean square displacement increases superlinearly with time  $\langle r^2 \rangle \sim t^\gamma$  for  $\gamma > 1$ . In this paper a superdiffusive process known as a Lévy walk, is used to analyze random scattering and growth in situations where Gaussian processes are not applicable. In a similar vein, the transmission probability of light through clouds has previously been analyzed as a non-Gaussian wave scattering process [5].

The origin of the differing behaviors, diffusive and superdiffusive, of Gaussian and Lévy processes is associated with the probability distributions of step lengths which make up the respective random walks. If the distribution of step lengths has a finite second moment (i.e., a variance) then the central limit theorem guarantees that the process is Gaussian [6]. Processes which exhibit superdiffusion have no second moment (i.e., infinite variance) and fail to satisfy the conditions of the central limit theorem. The finite second moment of a Gaussian process implies that the modeled system possesses a characteristic length scale of this order, whereas systems which can be modeled through Lévy processes possess

no such characteristic length scale. In order for the distribution of step lengths to have no second moment, the distribution must have a slowly decreasing tail; e.g., a power law tail with index  $\alpha$  such that  $1 < \alpha < 3$ . The lower limit on  $\alpha$  is imposed to ensure the probability distribution of step lengths can be normalized.

Two different superdiffusive Lévy random processes have been studied in the literature, Lévy flights and Lévy walks. Lévy flights were developed first and involve random walks steps occurring at regular times. Unfortunately, Lévy flights take arbitrarily large steps in finite times and thus the random walk involves arbitrarily large velocities. Lévy walks were explicitly developed to avoid this nonphysical aspect of Lévy flights. In a Lévy walk the time taken to complete each random walk step depends linearly on the length of that step. The lack of unphysical features makes Lévy walks the natural choice for modeling superdiffusive random walks in the context of random scattering and random growth in waves.

The purpose of this paper is to apply Lévy walk random processes to random wave scattering and growth. In Sec. II the basic evolution equations for Lévy walks are introduced. In Sec. III Lévy walks are used to model wave spatial scattering and then combined with wave growth at a constant growth rate. In Sec. IV waves with randomly varying growth rates which can be modeled as Lévy walks in gain are analyzed, first in the absence of spatial scattering (ballistic propagation) and then with Gaussian diffusive spatial scattering. In Sec. V waves are studied which are scattered according to Lévy processes while subject to randomly varying growth rates, which can be modeled as Lévy walks in gain.

**II. BASIC THEORY**

In this section we give the basic equations for the Lévy walk model in particular the so-called *velocity model* which we shall use to model both spatial diffusion and/or growth in this paper.

The Lévy walk can be visualized by considering a random walker whose walk consists of a series of steps between points known as turning points. In traveling between these turning points the random walker travels at constant velocity. When the random walker reaches a turning point, the length of the next step of the walk is chosen from a jump distribu-

\*Electronic address: P.Drysdale@physics.usyd.edu.au

†Electronic address: P.Robinson@physics.usyd.edu.au

tion  $\psi(x)$ . Thus, when the random walker is at a turning point, the probability the walker will end up at its next turning point a distance  $x$  away in a time  $t$ , is given by

$$\Psi(x,t) = \psi(x)\delta(|x| - vt). \quad (1)$$

It should be noted that in one dimension (1D) the random walker does not necessarily reverse direction at each turning point. For symmetric jump distributions, there is a 50% probability the next step will be in the same direction as the walker was traveling when it reached the turning point. For Lévy walks in spaces of higher dimension, turning points do correspond to spatial turns with unit probability. As stated in Sec. I, the Lévy walk is superdiffusive, so the jump distribution  $\psi(x)$  has a divergent second moment. For  $\psi(x)$  to be monotonically decreasing as a power law for large  $|x|$  and have a divergent second moment, we choose  $\psi(x)$  to have the form  $\psi(x) \sim |x|^{-\alpha}$  for large  $|x|$ , where  $1 < \alpha < 3$ . The index  $\alpha$  can then be used to classify Lévy walk processes.

We let  $Q(x,t)$  denote the probability distribution of turning points of the random walk. For a Lévy walk on a finite interval  $[0,L]$  with absorbing boundaries,  $Q(x,t)$  is given by

$$Q(x,t) = \int_0^L \int_0^t Q(x',t')\Psi(x-x',t-t')dx'dt' + \delta(x-x_0)\delta(t), \quad (2)$$

where  $x_0$  is the starting point of the random walk. Equation (2) links the current turning point distribution with those at previous times through the jump distribution. At any time the random walk is either at a turning point or traveling to the next turning point, so the probability distribution  $P(x,t)$  for the position of the random walker is

$$P(x,t) = \int_0^L \int_0^t Q(x',t')\Phi(x-x',t-t')dx'dt', \quad (3)$$

where  $\Phi(x,t)$  is the probability of walker being found on the way to the next turning point and is given by

$$\Phi(x,t) = \delta(|x| - vt) \int_{|x|}^{\infty} \psi(x')dx'. \quad (4)$$

The Laplace transform of the turning point distribution will be required in our analysis and is obtained by Laplace transforming Eq. (2), which yields

$$Q(x,s) = \int_0^L \Psi(x-x',s)Q(x',s)dx' + \delta(x-x_0). \quad (5)$$

Exact analytic solutions are not known for Eq. (5). However, since the properties of  $Q(x,t)$  are dependent on the positions and types of the singularities of  $Q(x,s)$  it is sufficient to know the solutions of the corresponding eigenvalue equation of Eq. (5), which is given by

$$Q(x,s) = \int_0^L \Psi(x-x',s)Q(x',s)dx'. \quad (6)$$

Like Eq. (5), no analytic solutions for the eigenvalue equation (6) are known. Given the fundamental importance of

understanding the solutions to Eq. (6) and to avoid other researchers being misled, we show in the Appendix that a tabulated, purported analytic solution of this eigenvalue equation is actually incorrect.

Despite the lack of closed solutions of the eigenvalue equation, some basic properties of  $Q(x,t)$  have been derived by considering the singularities of Eq. (5) [7]. In particular the singularities of  $Q(x,s)$  are simple poles lying on the negative real axis in the complex- $s$  plane. Each pole contributes a term exponentially decaying in time to  $Q(x,t)$ , so  $Q(x,t)$  and  $P(x,t)$  consists of the sum of a number of terms exponentially decaying in time. This is similar to Gaussian diffusion on an interval where the probability distribution is the sum of a number of exponentially decaying eigenfunctions. A crucial difference exists between Lévy walks on an interval and Gaussian diffusion on an interval. It should be noted that Eq. (6) is not strictly a single eigenvalue equation, but a set of equations, indexed by  $s$ . Thus each pole of  $Q(x,s)$  converges on an eigenfunction of a different eigenvalue equation. Thus  $Q(x,t)$  is the sum of decaying eigenfunctions from different eigenvalue equations [7]. Unlike the Gaussian case, the exponential decay constants of each of these eigenfunctions are not the eigenvalues [7]. The decay constants are given by the positions of the poles  $s_i$ , where poles are numbered in order of distance from the origin. To preserve analogies with Gaussian diffusion, it is convenient to term the value  $\Lambda_i = -s_i$  at each pole a pseudoeigenvalue and the spatial component of  $P(x,t)$  for each decaying term as a pseudoeigenfunction. The first pseudoeigenvalue scales with system size as  $s_1 \propto L^{1-\alpha}$  for  $2 < \alpha < 3$  and  $s_1 \propto 1/L$  for  $1 < \alpha < 2$  [7].

### III. LÉVY SPATIAL DIFFUSION WITH CONSTANT WAVE GROWTH RATE

Let us now consider a wave traveling through a medium. In general, the wave may either be scattered by the medium as it propagates or more simply propagate ballistically; i.e., remain unscattered by the medium. Similarly the wave can be amplified or damped by the medium in addition to its ballistic or scattered propagation. The scattering process may be modeled in two ways based on the distribution of scattering centers in the medium. As large steps between scattering events are rare, the scattering is most commonly modeled by Gaussian diffusion [3]. In a medium where large steps can occur between scattering, such as in clouds, the scattered path of the wave can be modeled by a Lévy walk. Thus three forms of spatial propagation can be described: ballistic, Gaussian scattered, and Lévy scattered. If the wave is amplified or damped by the medium, more than one model can be used to describe this process. Most simply, the wave can be subject to a constant linear wave growth rate. For an inhomogeneous medium, the wave growth rate may vary rapidly as the wave propagates. The variation in the wave growth rate may then be modeled as a random walk in the gain of the wave. As with spatial scattering the random walk in gain can be classified by the distribution of step sizes. A Lévy walk in gain would correspond to a medium where large changes in wave gain are relatively more probable than a

medium which is modeled by a Gaussian walk in gain.

In this section we consider a wave undergoing spatial scattering modeled by a Lévy walk which is amplified/damped by either a constant linear wave growth rate or amplification/damping involving a Gaussian random walk in gain.

Before considering the above situations, we briefly consider Lévy spatial scattering in the absence of any wave growth, using a Laplace transform approach. This approach has the advantage of readily generalizing to a system with constant wave growth rate.

### A. Transmission coefficient without wave growth

The transmission coefficient of a medium for an incident wave is generally understood to be the fraction of incident wave energy that ultimately passes out the far side of the medium. In the random walk model of scattering this corresponds to the fraction of random walkers injected at one boundary that emerge at the other. For Gaussian spatial scattering the transmission coefficient in the absence of wave growth is a classical result (see, for example, [3,8]) and scales with system size as

$$T \propto 1/L. \quad (7)$$

For a Lévy walk in spatial scattering in the absence of wave growth, the transmission coefficient is identical to the transmission coefficient for a Lévy flight, since the temporal differences between the two types of random walks do not affect the final numbers of random walkers ejected from each side of the medium. For a Lévy flight on a discrete lattice (so that flight lengths have integer values only), Kesten [9] obtained the transmission coefficient. Davis and Marshak [5] independently obtained the transmission coefficient for a continuous distribution flight steps in connection with light transmission through a cloudy atmosphere. The transmission coefficient scales in the same way in both cases and is given by

$$T \propto L^{(1-\alpha)/2}. \quad (8)$$

As might be expected, the transmission coefficient falls off more slowly with  $L$  for  $\alpha < 3$ , than for a Gaussian scattering medium due to the relatively higher probability of the wave traveling long distances in the medium without undergoing scattering.

We now approach this problem from a Laplace transform approach applied directly to the Lévy walk model. The transmission coefficient for a Lévy walk in the absence of growth is given by

$$T = \int_0^L dx' \int_0^\infty dt' Q(x', t') \int_L^\infty dx \int_{t'}^\infty dt \Phi(x - x', t - t'), \quad (9)$$

where  $\Phi(x, t)$  is defined in Eq. (4). Equation (9) can be understood as counting the fraction of random walkers which leave the system on the far side. The  $x$  and  $t$  integrals represent the probability that a walker at a turning point will leave the medium without further scattering. The integrals over  $x'$

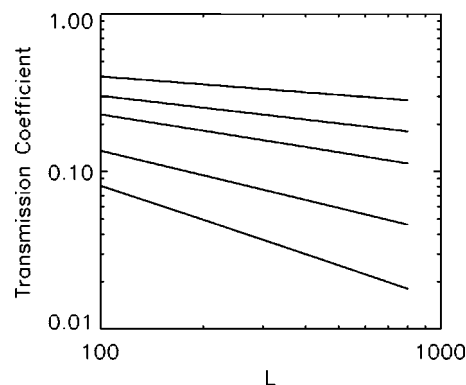


FIG. 1. Transmission coefficient vs  $L$ , as given by Eq. (17). From top to bottom the lines correspond to  $\alpha=1.3333, 1.5, 1.6666, 2.05, 2.5$ .

and  $t'$  sum these probabilities over all possible turning points. This expression can be rewritten in terms of the Laplace transforms of  $Q(x, t)$  and  $\Phi(x, t)$ , giving

$$T = \int_0^L Q(x', s=0) \Phi(L - x', s=0) dx', \quad (10)$$

where  $Q(x', s=0)$  is given by Eq. (5). To obtain the transmission coefficient numerically from Eq. (10), Eq. (5) is discretized using the Nystrom or product Nystrom methods [10] and a matrix inversion is performed to find  $Q(x, s=0)$ , the quadrature in Eq. (10) then gives  $T$ . Figure 1 show numerical computations of the transmission coefficient using this numerical scheme. The results in Fig. 1 agree with the previously known analytic form (8) [5,9,11]. Clearly for a system with no growth, the Laplace transform approach (which involves numerical computations) has no advantage over analytic solutions derived in the context of Lévy flights. Nonetheless, this analysis of the transmission coefficient in the absence of growth provides a simple illustration of the Laplace transform method which readily generalizes to systems with wave growth.

### B. Transmission coefficient with constant wave growth rate

In a system undergoing wave growth, the transmission coefficient may again be defined to be the relative fraction of incident energy that escapes on the far side of the medium. For  $\Gamma > 0$  we expect the sum of the reflection and transmission coefficients to exceed 1 as the system amplifies the incident wave. This is expected whether the system is subject to Lévy or Gaussian spatial scattering. Thus Eq. (65) of [3] was incorrect and the correction is that the inequality  $R + T < 1$  only applies for damped systems  $\Gamma < 0$ . Note, however, the correct signed result  $|R - T| \leq 1$  is implicitly shown in 2. 2 of that paper.

In a system where wave growth occurs at a constant growth rate of  $\Gamma$  the transmission coefficient is modified to the form

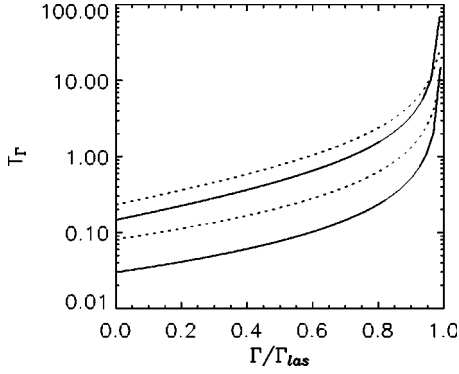


FIG. 2. Transmission coefficient  $T_\Gamma$  vs  $\Gamma/\Gamma_{las}$ , as given by Eq. (12). From top to bottom the lines correspond to  $L=100, 400$  with  $\alpha=1.6666$ ;  $L=100, 400$  with  $\alpha=2.5$ ,  $\psi(x)=C(\alpha)(1+x^2)^{-\alpha/2}$ .

$$T_\Gamma = \int_0^L dx' \int_0^\infty dt' Q(x', t') \int_L^\infty dx \int_{t'}^\infty dt \Phi(x-x', t-t') e^{\Gamma t_0}, \quad (11)$$

where  $t_0$  is the time before leaving the edge of the medium; i.e.,  $t_0 = t' + (L-x')/v$ , corresponding to the sum of the time taken to reach the final turning point at  $(x', t')$  and the time taken to travel between this turning point and escape at the medium edge. Equation (11) can be simplified to yield

$$T_\Gamma = \int_0^L Q(x', s = -\Gamma) e^{\Gamma(L-x')/v} \Phi(L-x', s=0) dx'. \quad (12)$$

Wave energy injected into a Gaussian spatial scattering medium without growth escapes the medium, the energy remaining in the medium [survival probability  $\Theta(t)$ ] is given by a sum of exponentially decaying terms, the longest lived of which decays as  $e^{-\lambda_1 t}$ , where  $\lambda_1$  is the first eigenvalue. If the system now includes amplification at a constant wave growth rate  $\Gamma$ , the longest lived term will decay as  $e^{(\Gamma-\lambda_1)t}$ . The medium will lase if  $\Gamma > \lambda_1$ , and  $\lambda_1$  is thus the lasing threshold for the system, as found by Letokhov [4]. Similarly for a spatially Lévy scattering medium, a threshold growth rate exists beyond which the medium lases. As previously described, for wave energy injected into a Lévy scattering medium without growth the survival probability can be expressed as the sum of a number of exponentially decaying terms, the longest lived of which has a decay rate equal to the first pseudoeigenvalue  $\Lambda_1$ . Thus, as for Gaussian scattering, the medium will be expected to lase when the exponential growth rate exceeds the longest lived decaying pseudoeigenstate; i.e.,

$$\Gamma_{las} = \Lambda_1, \quad (13)$$

where  $\Lambda_1$  is the first pseudoeigenvalue of the Lévy scattering medium. This lasing threshold appears naturally in Eq. (12) via the divergence of  $Q(x, s)$  at its first singularity along the negative real axis at  $s = -\Lambda_1$ .

Although, formally, the lasing threshold differs little from Letokhov's result for Gaussian scattering, we note its scaling with system size differs markedly due to the different scaling of the eigenvalues and pseudoeigenvalues with  $L$ . For Gaussian scattering  $\Gamma_{las} \propto L^{-2}$ , whereas for Lévy scattering

$$\Gamma_{las} \propto \begin{cases} L^{1-\alpha}, & 2 < \alpha < 3, \\ L^{-1}, & 1 < \alpha < 2. \end{cases} \quad (14)$$

Having established the location of the lasing threshold, the properties of  $T_\Gamma$  can be considered. Trivially, for  $T_\Gamma$  near the lasing threshold  $T_\Gamma \propto 1/(\Lambda_1 - \Gamma)$  asymptotically, just as for Gaussian scattering media. This is the contribution to  $T_\Gamma$  of the longest lived exponentially decaying first pseudoeigenstate decaying with rate  $(\Lambda_1 - \Gamma)$ . The first pseudoeigenstate is the only divergent term contributing to  $T_\Gamma$ . Figure 2 shows  $T_\Gamma$  for different  $\alpha$  and  $L$  calculated numerically. A general trend of an approximately exponential increase for small  $\Gamma$  before increasing asymptotically near the lasing threshold can be seen.

### C. Wave energy density in medium

We now consider the distribution of photons in the medium subject to continuous injection of photons within the medium. Continuous injection into a scattering medium in the absence of growth will be considered first.

For Gaussian scattering the distribution of photons forms a triangular distribution given by

$$P(x) = \frac{2L}{D_{xx}} \times \begin{cases} \frac{x_0}{L} \left(1 - \frac{x}{L}\right), & x_0 < L, \\ \frac{x}{L} \left(1 - \frac{x_0}{L}\right), & x_0 > L. \end{cases} \quad (15)$$

This is a corrected form of the result stated in Eqs. (30)–(32) of [3], where the result quoted in that paper has been multiplied by a missing factor of  $L^2$  in order to scale correctly with scattering medium length.

For Lévy scattering, the probability distribution inside the medium, under continuous injection, is obtained by integrating over all time the probability distribution  $P(x, t)$  for a system which evolves from a single one-off injection of photons. By Laplace transforming Eq. (3) and noticing  $P(x, s=0)$  corresponds to the integral over all time of  $P(x, t)$ , we have

$$\int_0^\infty P(x, t) dt = P(x, s=0), \quad (16)$$

$$= \int_0^L \Phi(x-x', s=0) Q(x', s=0) dx'. \quad (17)$$

The asymptotic form for  $P(x, s=0)$  as  $\alpha \rightarrow 1$  can be immediately obtained by observing  $\Phi(x, s=0) \rightarrow \text{constant}$  in this limit, so Eq. (17) predicts  $P(x, s=0) \rightarrow \text{constant}$  as  $\alpha \rightarrow 1$ .

To obtain  $P(x, s=0)$ , Eq. (5) is inverted numerically to obtain  $Q(x, s=0)$  and the convolution in Eq. (17) is performed to yield the probability distribution inside the me-

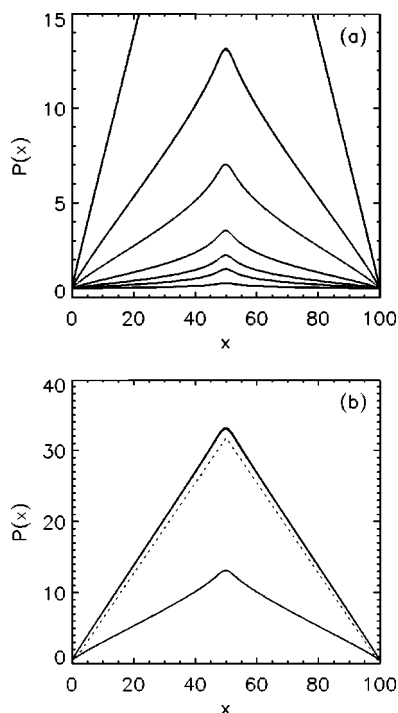


FIG. 3. Distribution of wave energy  $P(x)$  inside medium with continuous injection as given by Eq. (17) for  $L=100$ ,  $\psi(x) = C(\alpha)(1+x^2)^{-\alpha/2}$ . From bottom to top the curves correspond to (a)  $\alpha=1.15, 1.5, 1.75, 2.05, 2.5, 2.95, 4.0$  ( $\alpha=4.0$  is truncated) and (b)  $\alpha=2.95, 4.0$ . The dotted curve in (b) is  $P(x)$  in the Gaussian diffusive limit ( $\sigma^2 \ll L$ ) given by Eq. (15).

dium. Another method for obtaining  $P(x, s=0)$  is a direct Monte Carlo simulation of the Lévy walk, which is then integrated over all time. Despite the Monte Carlo scheme scaling computationally as  $N^\beta$  with  $\beta = \max(2, \alpha)$ , while the matrix inversion in the Laplace space approach scales as  $N^{\log_2 L} \approx N^{2.8}$  [10], the higher computational overheads for the Monte Carlo approach mean the Laplace approach is significantly superior for  $\alpha < 2.8$  even for moderately large  $L$ , such as the range  $100 < L < 800$  for which we have performed computations.

Figure 3 shows  $P(x, s=0)$  for various  $\alpha$  using the Laplace space numerical approach described above. As  $\alpha$  decreases from 3 to 1,  $P(x, s=0)$  shows a continuous deformation from the triangular Gaussian limit to the constant distribution as  $\alpha \rightarrow 1$ . Even at  $\alpha=2.5$  the probability distribution can be well approximated by a triangular distribution over 80% of its length. The largest differences between the probability distribution and a triangular distribution occur near the injection point. At  $\alpha=2.5$  the lowest order pseudoeigenfunctions and pseudoeigenvalues still closely resemble their Gaussian counterparts whereas the higher order pseudoeigenfunctions differ more significantly from the Gaussian limit [7]. Since the higher order pseudoeigenfunctions, define the shape of  $P(x, s=0)$  near the injection point, it is to be expected that  $P(x, s=0)$  will be similar to the Gaussian limit except near the injection point.

For a Gaussian scattering medium, the distribution of last scattering points before the photon leaves the medium is localized in the vicinity of the edges. For a Lévy scattering

medium, as  $\alpha$  decreases the distribution of last scatter points becomes more concentrated near the injection point as will now be demonstrated. As  $\alpha$  decreases,  $\Phi(x, s=0)$  takes a flattened functional form approaching a constant in the limit  $\alpha \rightarrow 1$ . As a consequence  $\Phi(x, s=0)$  dominates the convolution in Eq. (17), so  $P(x, s=0)$  takes a more uniform distribution and is not strongly dependent on the functional form of the turning point distribution  $Q(x, s=0)$ . A number of physical insights may be deduced from these relationships. As  $\alpha$  decreases the probability distribution for finding photons  $P(x, s=0)$  becomes more uniform. The dominant contribution of  $\Phi(x, s=0)$  to  $P(x, s=0)$  indicates the probability of finding a photon at a particular location is dominated by photons which have left their final turning point (i.e., last scatter point) and are taking their final walk step that leads them out of the medium. The scattering in the medium is not more evenly distributed because of the fact that the turning point distribution remains strongly peaked. Further, as  $\alpha \rightarrow 1$ , the distribution of last scatter points becomes concentrated near the injection point where the turning point distribution is peaked, rather than near the edges, as would be the case for Gaussian scattering.

Up to this point we have considered the injection of photons in equal numbers in each direction at the injection point within the medium. In the Gaussian scattering case, if the injection of photons is outside the medium, the *diffusive approximation* is made where the photons are assumed to propagate ballistically to a point of first scattering roughly one mean free path into the medium and then undergo pure diffusion [3]. Similarly injection in only one direction of photons within the medium will result in ballistic propagation followed by pure diffusion. For most purposes it may be assumed the ballistic propagation distance is small and there is little difference between the two types of initial conditions regardless of the injection point. For Lévy scattering systems, the absence of a characteristic scattering length scale means no diffusive approximation can be made. For injection of photons from outside the medium, this can be trivially accommodated by using the initial condition  $2\delta(x-x_0)\delta(t)$  for  $x_0 \rightarrow 0$ . Unidirectional injection inside the medium requires changing the initial conditions in Eq. (5) to  $H(x-x_0)\psi(x-x_0)$  where  $H$  is the Heaviside function. The probability distribution under continuous unidirectional injection is skewed toward the direction of injection.

Having considering the continuous injection system in the absence of wave growth, wave growth can be introduced by analogy to Eq. (17), yielding

$$W(x, \Gamma) = \int_0^\infty P(x, t) e^{\Gamma t} dt, \quad (18)$$

$$= P(x, s = -\Gamma), \quad (19)$$

$$= \int_0^L \Phi(x-x', s = -\Gamma) Q(x', s = -\Gamma) dx, \quad (20)$$

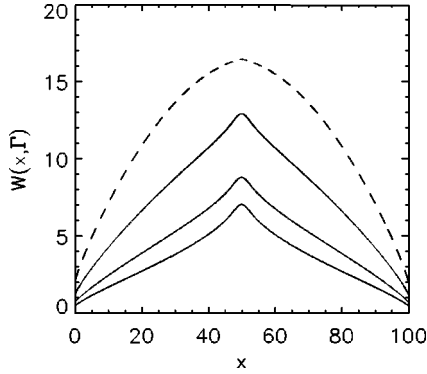


FIG. 4. Wave energy density  $W(x, \Gamma)$  vs  $x$ , as given by Eq. (21), for  $\alpha=2.5$ ,  $\psi(x)=C(\alpha)(1+x^2)^{-\alpha/2}$ . From bottom to top, the curves are  $\Gamma=0, 0.001, 0.002$ . The dashed curve shows  $0.2W(x, \Gamma)$  for  $\Gamma=0.0035$ .

$$= \int_0^L dx' e^{\Gamma|x-x'|} Q(x', s=-\Gamma) \int_{|x-x'|}^{\infty} \psi(x'') dx'' \quad (21)$$

Numerically inverting Eq. (5) and performing the convolution in Eq. (21) enables us to find the probability distribution inside the medium for each particular  $\alpha$  and  $\Gamma$ . Considering first  $P(x, \Gamma)$  for  $2 < \alpha < 3$ , Fig. 4 shows the probability distributions as  $\Gamma$  is varied from no growth to the lasing threshold. The general trend in this figure is reflected over the whole range  $2 < \alpha < 3$  and shows the probability distribution starting from the triangle-like distribution in the absence of growth and smoothly deforming to the sinelike shape of the first pseudoeigenfunction. This behavior is very similar to the behavior of Gaussian systems, in which  $P(x, \Gamma)$  varies smoothly from the purely triangle distribution (15) to the sine form of their first eigenfunction as the lasing threshold is approached [3]. The reasons for this behavior are exactly the same as those for the asymptotic dominance of the first pseudoeigenfunction in the transmission coefficient  $T_\Gamma$ . The first pseudoeigenfunction contributes a diverging component to the overall distribution  $P(x, \Gamma)$  as  $\Gamma \rightarrow \Lambda_1$ .

Figure 5 shows a typical set of probability distributions  $P(x, \Gamma)$  as the growth rate is varied for  $\alpha=1.5$ . As before, the

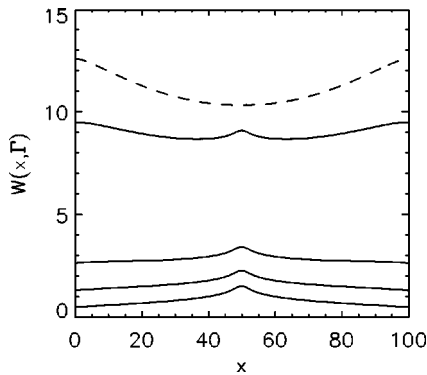


FIG. 5. Wave energy density  $W(x, \Gamma)$  vs  $x$ , as given by Eq. (21), for  $\alpha=1.5$ ,  $\psi(x)=C(\alpha)(1+x^2)^{-\alpha/2}$ . From bottom to top, the curves are  $\Gamma=0, 0.001, 0.015, 0.02$ . The dashed curve shows  $0.04W(x, \Gamma)$  for  $\Gamma=0.0225$ .

probability distribution changes from the no-growth case (in this case a relatively flat distribution) to approach the first pseudoeigenfunction which has upturned edges. Physically, the probability distribution is dominated by photons in the final walk step out of the medium which are multiplying exponentially along this final walk step, leading to the upturned peaks of the probability distribution approaching the boundaries of the medium. At this point it is useful to consider the general shape of the first pseudoeigenfunction in the range  $1 < \alpha < 2$ . In a paper on Lévy walks [7], we showed a set of first pseudoeigenfunctions for  $\alpha=1.75$  in Fig. 10(b) of that paper. Each showed simple concave-down curves. Thus we can deduce for  $\alpha=1.75$ ,  $P(x, \Gamma)$  would approach these curves as  $\Gamma \rightarrow \Lambda_1$ . As  $\alpha$  decreases, the concavity of the first pseudoeigenfunction reverses, having upturned edges as in the case  $\alpha=1.5$ . This reversal of the concavity of the first pseudoeigenfunction as  $\alpha$  decreases from 1.75 to 1.5, was not described in the earlier paper. The reason for the reversal is due to  $\Phi(x, s=-\Gamma)$  becoming U shaped rather than strongly peaked as for larger  $\alpha$ . In particular the shape of  $\Phi(x, s=-\Gamma)$  depends on the product  $s_1 L$ . For  $2 < \alpha < 3$ ,  $s_1 L$  scales as  $L^{\alpha-2}$  and thus the exponential term in  $\Phi(x, s=-\Gamma)$  remains small and  $\Phi(x, s=-\Gamma)$  is sharply peaked around  $x=0$ . For  $1 < \alpha < 2$ ,  $s_1 L$  is constant but the constant value increases from near one toward ten, as shown in Fig. 4(b) of [7]. Between  $\alpha=1.75$  with  $s_1 L \approx 1.4$  and  $\alpha=1.5$  with  $s_1 L \approx 2.1$ , the exponential term dominates  $\Phi(x, s=-\Gamma)$ , which becomes U shaped. The first pseudoeigenfunction then reverses concavity when the U-shaped  $\Phi(x, s=-\Gamma)$  dominates the turning point distribution  $Q(x, s=-\Gamma)$ .

#### IV. LÉVY WALK IN GAIN

In this section we consider the case of a Lévy walk in wave growth in the absence of spatial scattering and then coupled with Gaussian spatial diffusion. In analyzing stochastic wave growth, Robinson [3] assumed that the growth rate of a wave can undergo a Gaussian random walk in gain. Interestingly, such a wave can undergo net wave growth even if the mean growth rate is negative. In this section we generalize the theory of stochastic wave growth to a wave undergoing a Lévy walk in gain.

##### A. Lévy walk in gain with ballistic propagation

Assuming the Lévy walk in gain is unbounded, the mean energy density in the wave in the absence on spatial scattering can be given simply by

$$\langle W(t) \rangle = \int_{-\infty}^{\infty} e^G p(G - \langle G(t) \rangle, t) dG, \quad (22)$$

where  $p(G - \langle G(t) \rangle, t)$  is the probability distribution of an unbounded Lévy walk centered on a mean gain  $\langle G(t) \rangle = \langle \Gamma \rangle t$ . For Lévy walks in gain, the velocity of the Lévy walk shall be denoted  $\gamma$  to distinguish it from the velocity  $v$  of spatial Lévy walks.

It is preferable to use a Lévy walk rather than a Lévy flight, not only as it avoids the unbounded velocity which

occurs during large steps of a Lévy flight, but also after one step a Lévy flight in gain results in a divergent wave power because arbitrarily large steps are allowed in finite times. Zumofen and Klafter [12] obtained useful approximate forms for  $p(x,t)$ , the unbounded Lévy walk, in Fourier/Laplace space and real space. Here these form the basis for obtaining the mean energy density for waves undergoing a Lévy walk in gain. These results are then compared to  $\langle W(t) \rangle$  for waves where the Lévy walk in gain is obtained through Monte Carlo simulations. Given the different functional forms for the unbounded Lévy walk for  $1 < \alpha < 2$  and  $2 < \alpha < 3$  we shall consider each parameter range separately.

For an unbounded Lévy walk with velocity to unity and index  $2 < \alpha < 3$ , Zumofen and Klafter [12] showed the probability distribution was related to the Lévy distribution and is given by

$$P(x,t) = \begin{cases} a_0 t^\beta \exp[-a_1 \{x/t^\beta\}^2], & x \ll t^\beta, \\ b t x^{-\alpha}, & t^\beta \ll x < t, \\ 0, & x > t, \end{cases} \quad (23)$$

where  $\beta = (\alpha - 1)^{-1}$ . By substituting  $P(x,t)$  in a form where velocity has not been normalized directly into Eq. (22), the mean energy density for large times can be approximated by its dominant term as

$$\langle W(t) \rangle \approx b e^{(\Gamma + \gamma)t} (\gamma t)^{1-\alpha}. \quad (24)$$

For an unbounded Lévy walk with index  $1 < \alpha < 2$ , the probability distribution is not connected to the Lévy distribution. Zumofen and Klafter obtained an approximate analytic form for the probability distribution for a Lévy walk in this regime [12]. When expressed in units where velocity has not been normalized to unity, their Eq. (81) can be written

$$P(k,s) = \frac{1}{\gamma} \frac{(s/\gamma + ik)^{\alpha-2} + (s/\gamma - ik)^{\alpha-2}}{(s/\gamma + ik)^{\alpha-1} + (s/\gamma - ik)^{\alpha-1}}. \quad (25)$$

Except in the special case  $\alpha = 3/2$  [12], there is no known closed analytic form for the probability distribution in real space. Nonetheless, we can use operator identities to obtain the asymptotic time behavior of  $\langle W(t) \rangle$ , which is done next. The justification for this method is given when we compare our results with Monte Carlo simulations below.

Noting that Eq. (22) may be rewritten formally as

$$\langle W(t) \rangle = e^{G(t)} P(k = -i, t), \quad (26)$$

we require the time asymptotic properties of

$$P(k = -i, s) = \frac{(s + \gamma)^{\alpha-2} + (s - \gamma)^{\alpha-2}}{(s + \gamma)^{\alpha-1} + (s - \gamma)^{\alpha-1}}. \quad (27)$$

Theorem 13.7 of Doetsch [13], connects the time asymptotic properties of a function with the form of the Laplace transform near the singular point with the largest real part. The transform  $P(k = -i, s)$  satisfies the constraints of this theorem and the asymptotic properties may be deduced by completing the complex path integral around the singularity at  $s = \gamma$  in the way described by Doetsch. Near  $s = \gamma$ ,  $P(k = -i, s)$  has the form

$$P(k = -i, s) \approx (2\gamma)^{1-\alpha} (s - \gamma)^{\alpha-2}, \quad (28)$$

whence the asymptotic form is

$$P(k = -i, t) \approx \frac{1}{2^{\alpha-1} \Gamma_E(2-\alpha)} e^{\gamma t} (\gamma t)^{1-\alpha}, \quad (29)$$

where  $\Gamma_E$  is Euler's gamma function (subscripted to distinguish it from the wave growth rate). Thus the mean energy density is given by

$$\langle W(t) \rangle = \frac{1}{2^{\alpha-1} \Gamma_E(2-\alpha)} e^{(\Gamma + \gamma)t} (\gamma t)^{1-\alpha}, \quad (30)$$

which is of the same functional form as the mean energy density for the range  $2 < \alpha < 3$ .

As noted previously, for  $\alpha = 3/2$  the probability distribution has an analytic form in real space [12] and the mean energy density can be calculated directly from Eq. (22). The probability distribution is given by

$$P(x,t) = \begin{cases} \pi^{-1} [(\gamma t)^2 - r^2]^{-1/2}, & r < \gamma t, \\ 0, & r > \gamma t. \end{cases} \quad (31)$$

Thus the mean energy density of the wave is

$$\langle W(t) \rangle = \exp(\langle \Gamma \rangle t) I_0(\gamma t), \quad (32)$$

where  $I_0$  is a Bessel function of imaginary argument. For large times this approaches the asymptotic form and normalization obtained from by the operator technique for  $1 < \alpha < 2$  given in Eq. (30).

It is important to consider the accuracy of the mean energy densities obtained above. The major difficulty with the above analysis is that the Lévy walk distributions used are only approximate forms, which provide a good approximation of the Lévy walk distribution  $P(x,t)$  over much of its range [12], but are not exact. For the purposes of calculating the mean energy density of a wave undergoing a Lévy walk in gain, only the vicinity of  $x = \gamma t$  contributes significantly to the mean energy density. This is exactly where the approximate forms are known to deviate from the true distribution, and thus the use of these approximate forms for the Lévy walk distributions is not ideal in these circumstances. The mean energy densities calculated above were compared to mean energy densities calculated by numerically integrating Eq. (22) where the Lévy walk distribution was obtained from Monte Carlo simulations. The comparison showed that the functional form of the asymptotic scaling in Eqs. (24) and (30) is correct but the proportionality constants disagree. For  $2 < \alpha < 3$ , a further refinement to the analytic proportionality factor  $b = 1/[2\zeta(\alpha-1)]$  [where  $\zeta(x)$  is the Riemann zeta function] can be made by recognizing at  $x = \gamma t$  the Lévy distribution has sharp ballistically propagating peaks which includes walkers which have never been scattered. These peaks are not included in the estimate of  $P(x,t)$  given in Eq. (23). The ballistic peaks can be seen in simulations of  $P(x,t)$  such as Fig. 9 9 of [7]. Incorporating the walkers which have never been scattered yields a refined estimate for the proportionality factor of

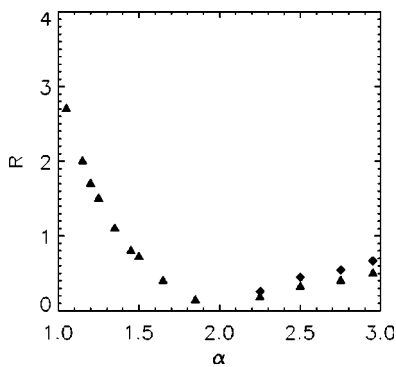


FIG. 6. The ratio  $R$  of the proportionality constants of the analytic time asymptotic form to the numerically evaluated mean energy density for a Lévy walk in gain. The ratio shown in diamonds incorporates the refined analytic approximation given by Eq. (33) which includes the effect of the ballistic peaks for  $2 < \alpha < 3$ .

$$1/[2\zeta(\alpha - 1)] + b/(\alpha - 1). \tag{33}$$

This refinement provides only moderate improvement in the agreement of the proportionality factor.

Figure 6 shows the ratio of the analytically obtained proportionality factors given in Eqs. (24) and (30), divided by the observed proportionality factor of the asymptotic form obtained from Monte Carlo simulations yielding  $\langle W(t) \rangle$ . Although other refinements for approximating these proportionality constants have been considered, the large overheads that such techniques require and the relatively small improvements gained, suggest that Monte Carlo simulations are the most efficient method for obtaining accurate values of these constants if required.

Some conclusions regarding wave growth involving Lévy walks in gain can now be drawn. As with waves growing with a Gaussian random walk in gain, the wave may undergo net wave growth even though the mean wave growth is negative if  $\gamma > \langle \Gamma \rangle$ . For a Gaussian diffusive random walk in gain, the wave grows exponentially in time with a mean wave growth rate given by  $\Gamma_{\text{eff}} = \langle \Gamma \rangle + \sigma^2(\Gamma)t_{\Gamma}$  [3]. For a Lévy walk in gain, the mean energy density increases asymptotically as  $\langle W(t) \rangle \propto (\gamma t)^{1-\alpha} \exp(\langle \Gamma \rangle t + \gamma t)$ , rather than exponentially. In the Gaussian case the effective wave growth rate depends on the width of  $P(G, t)$  through the standard deviation  $\sigma$ , a much smaller parameter than the velocity of the Lévy walk  $\gamma$ . As expected, the mean energy density for a Lévy walk in gain still increases faster than the Gaussian case despite the power law weighting term  $(\gamma t)^{1-\alpha}$  since the coefficient within its exponential term is larger than the coefficient in the Gaussian case. For Lévy walks the term  $\exp(\langle \Gamma \rangle t + \gamma t)$  in the asymptotic form depends on the velocity of the Lévy walk, not the behavior of the rest of the probability distribution. Not unexpectedly it is the largest steps of the Lévy walk that determine the dominant evolution of  $\langle W(t) \rangle$ .

The Gaussian walk in gain based on the velocity model where  $\psi(x)$  has a power law tail of index  $\alpha > 3$  must be considered carefully. This system is different from the Gaussian diffusive random walk in gain analyzed in [3] as velocity model Gaussian walks are not equivalent to Gauss-

ian diffusive random walks. For a velocity model Gaussian walk with a power law tail, the mean energy density has a term  $(\gamma t)^{1-\alpha} \exp(\langle \Gamma \rangle t + \gamma t)$  which increases faster than the term  $\exp[\langle \Gamma \rangle + \sigma^2(\Gamma)t_{\Gamma}]$ . Gaussian random walks with power law tails ( $\alpha > 3$ ) have slow convergence to behavior predicted by diffusion equations for points far from the center of the walk. This yields discrepancies such as observed here.

### B. Lévy walk in gain coupled with Gaussian spatial scattering

We turn now to waves which undergo a Lévy random walk in gain and Gaussian spatial scattering. In the absence of the random walk in gain, the probability distribution is well known (e.g., [3,14]) with:

$$P_G(x, t) = 2 \sum_{n=1}^{\infty} e^{-\lambda_n t} \sin(n\pi x/b) \sin(n\pi/b). \tag{34}$$

The situation of a Gaussian random walk in gain coupled with Gaussian spatial scattering was considered by Robinson [3] and in this subsection we shall term this the ‘‘Gaussian’’ case for comparison purposes. With the Lévy random walk in gain coupled to Gaussian spatial diffusion, the mean energy density  $W(x)$  in the scattering medium is given by

$$W(x) = \int_0^{\infty} dt P_G(x, t) \int_{-\infty}^{\infty} dG e^G P(G - \langle G(t) \rangle, t). \tag{35}$$

Qualitatively several properties of  $W(x)$  can be deduced by considering Eq. (35). The integral in Eq. (35) converges only below a lasing threshold  $\langle \Gamma \rangle + \gamma < \lambda_1$ , just as the Gaussian case has a lasing threshold  $\langle \Gamma \rangle + \sigma^2(\Gamma)t_{\Gamma} < \lambda_1$  [3]. The lasing threshold for the Lévy case is independent of  $\alpha$ , the index of the Lévy walk over the whole range  $1 < \alpha < 3$ .

In the Gaussian case, the mean energy density  $W(x)$  smoothly changes from the triangular energy density profile (15) in the no growth case to the first eigenfunction of the diffusive system,  $\sin(n\pi x/b)$ , as the lasing threshold is approached [3]. For Lévy walks in gain, qualitatively different behavior for  $W(x)$  is expected for each of the cases  $1 < \alpha < 2$  and  $2 < \alpha < 3$ . The longest lived term and thus the term with the largest contribution to the time integral in Eq. (35) is due to the first eigenfunction of the diffusive system, whose time dependent component for large times is asymptotically

$$T_1 \sim (\gamma t)^{1-\alpha} e^{(\langle \Gamma \rangle + \gamma - \lambda)t}. \tag{36}$$

For  $1 < \alpha < 2$ , integrating this term over all time contributes a diverging term as the lasing threshold is approached. Like the Gaussian case,  $W(x)$  for  $1 < \alpha < 2$  smoothly changing from the triangular energy density profile (15) in the no-growth case to the first eigenfunction as the lasing threshold is approached. The divergent contribution of the first eigenfunction term implies  $W(x)$  diverges asymptotically as the lasing threshold is approached. For  $2 < \alpha < 3$  the situation is very different, the integral over the term (36) does not diverge and so the contribution of the first eigenfunction can never become dominant. Thus it can be concluded the mean energy density does not asymptotically diverge as the lasing



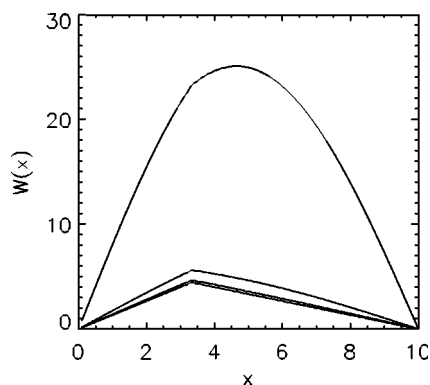


FIG. 7. Wave energy density  $W(x)$  vs  $x$ , as given by Eq. (35).  $P(G, t)$  was obtained by Monte Carlo simulations, for  $\alpha = 1.5$ ,  $\psi(x) = C(\alpha)(1+x^2)^{-\alpha/2}$ ,  $x_0 = 3.3$ , and  $\langle \Gamma \rangle = 0$ . From bottom to top, curves are  $\gamma/\lambda_1 = 0, 0.3, 0.6, 0.99$ .

threshold is approached and  $W(x)$  does not approach the first eigenfunction in this limit.

Analytic approximations to  $W(x)$  are difficult to obtain as these require accurate forms for  $\langle W(s) \rangle$  the Laplace transformed mean energy density of a Lévy walk in gain in the absence of spatial scattering, the situation analyzed in Sec. IV A. For  $1 < \alpha < 2$ , Zumofen and Klafter's approximate form for  $P(k, s)$  can be used to estimate  $W(x)$ . Equation (35) may be rewritten as

$$\begin{aligned}
 W(x) &\approx 2 \sum_{n=1}^{\infty} \sin(n\pi x_0/b) \sin(n\pi x/b) \\
 &\quad \times P(k = -i, s = \lambda_n - \langle \Gamma \rangle), \quad (37) \\
 &= 2 \sum_{n=1}^{\infty} \frac{(\lambda_n - \langle \Gamma \rangle + \gamma)^{\alpha-2} + (\lambda_n - \langle \Gamma \rangle - \gamma)^{\alpha-2}}{(\lambda_n - \langle \Gamma \rangle + \gamma)^{\alpha-1} + (\lambda_n - \langle \Gamma \rangle - \gamma)^{\alpha-1}} \\
 &\quad \times \sin\left(\frac{n\pi x_0}{b}\right) \sin\left(\frac{n\pi x}{b}\right). \quad (38)
 \end{aligned}$$

This approximate expression is the Lévy walk analogy to Eq. (72) in [3]. Qualitatively this expression shows the expected trends described in the previous paragraph. However, the caveats on the asymptotic forms derived in Sec. IV A apply to this expression, which is thus not a satisfactory method for obtaining quantitatively correct values for  $W(x)$ .

Numerical calculations are the preferable way of obtaining  $W(x)$ , which can be obtained by calculating  $P(G, t)$  via Monte Carlo simulations and then direct integration of Eq. (35). For  $1 < \alpha < 2$ , Fig. 7 shows  $W(x)$  obtained from Monte Carlo simulations and is consistent with the qualitative trends described above. The qualitative similarities in the trends for  $W(x)$  for  $1 < \alpha < 2$  and the Gaussian case can be seen by comparison with Fig. 4 of [3]. For  $2 < \alpha < 3$ , Fig. 8 shows  $W(x)$  obtained from Monte Carlo simulations. As expected from the qualitative discussion,  $W(x)$  does not diverge as  $\gamma$  approaches the lasing threshold and does not approach the first eigenfunction. The growth of  $W(x)$  as  $\gamma$  increases is also reduced relative to the range  $1 < \alpha < 2$ ,

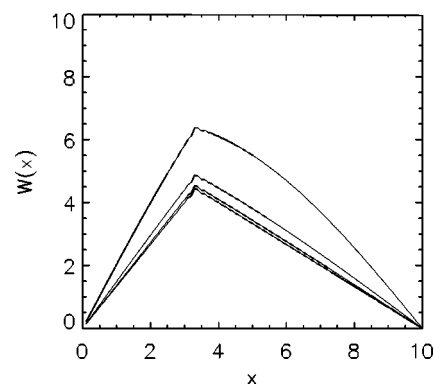


FIG. 8. Wave energy density  $W(x)$  vs  $x$ , as given by Eq. (35).  $P(G, t)$  was obtained by Monte Carlo simulations, for  $\alpha = 2.5$ ,  $\psi(x) = C(\alpha)(1+x^2)^{-\alpha/2}$ ,  $x_0 = 3.3$ , and  $\langle \Gamma \rangle = 0$ . From bottom to top, curves are  $\gamma/\lambda_1 = 0, 0.3, 0.6, 0.99$ .

reflecting the reduced probability of large steps in gain for the range  $2 < \alpha < 3$ . At first sight it may seem counterintuitive that  $W(x)$  does not asymptotically diverge near the lasing threshold for  $2 < \alpha < 3$  even though it does diverge in the Gaussian case. This is not a contradiction as the lasing threshold discontinuously changes from dependence on the velocity of the Lévy walk to dependence on the width of the probability distribution  $\sigma$  in the Gaussian case. This ensures that, for each  $\gamma$ ,  $W(x)$  is larger for the Lévy walk than for a Gaussian system, in accordance with intuitive expectations.

Similar numerical calculations can be used to obtain the transmission coefficient  $T_\Gamma$  for different  $\alpha$ , as shown in Fig. 9. As with  $W(x)$ , the transmission coefficient diverges near the lasing threshold for  $1 < \alpha < 2$  but remains finite for  $2 < \alpha < 3$ .

## V. LÉVY SPATIAL DIFFUSION WITH A LÉVY WALK IN GAIN

This section combines Lévy processes in scattering and in random wave growth. The wave entering the scattering medium is spatially scattered through a Lévy process while si-

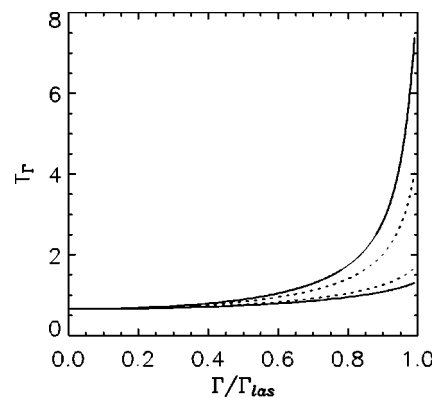


FIG. 9. Transmission coefficient  $T_\Gamma$  vs  $\Gamma/\Gamma_{las}$ . From top to bottom the lines correspond to  $\alpha = 1.5, \alpha = 1.75, \alpha = 2.25$ , and  $\alpha = 2.5$ .  $P(G, t)$  was obtained by Monte Carlo simulations, with  $\psi(x) = C(\alpha)(1+x^2)^{-\alpha/2}$ .

multaneously being subject to randomly varying wave growth as it propagates through the medium. This random variation in wave growth is modeled as a Lévy walk in gain which was introduced in Sec. IV A.

The chief difficulty of analyzing Lévy walks in gain coupled with Lévy spatial diffusion is that exact analytic forms for the probability distributions are not available for either the Lévy walk in gain or the Lévy scattering in the medium. Nonetheless, the essential properties of both these distributions are sufficiently well understood to build a clear picture of this system by considering aspects of previously analyzed cases in this paper.

The longest lived term of the Lévy spatial scattering is an exponential decaying term  $e^{-\Lambda_1 t}$ . By analogy to Sec. IV B the system has a lasing threshold given by  $\langle \Gamma \rangle + \gamma = \Lambda_1$ , where  $\Lambda_1$  is the first pseudoeigenvalue of the spatial scattering medium. The lasing threshold is independent of the index  $\alpha_{\text{gain}}$  of the Lévy walk in gain but indirectly dependent on the Lévy index of the spatial scattering  $\alpha_{\text{spatial}}$  which enters the threshold through  $\Lambda_1 = -s_1$ .

The nonexponential nature of the wave growth from the Lévy walk in gain prevents the use of the Laplace operator approach of Sec. III for determining the transmission coefficients and mean energy density in the medium. In the asymptotically large time limit, the functional form  $t^{1-\alpha} e^t$  for the growth of the Lévy walk in gain [Eqs. (24) and (30)] might suggest fractional differentiation in Laplace space to obtain the growth weighted probability distributions (see [15] for properties of fractional derivatives in Laplace space). This approach is not considered here as the nonlocal nature of fractional derivatives requires multiple numerical inversions of Eq. (5) which would be computationally inferior to Monte Carlo simulations unless an analytic solution to Eq. (5) can be found.

For  $1 < \alpha < 2$ , the transmission coefficient for the system rises from the no-growth case, diverging near the lasing threshold with an asymptotic scaling  $T_\Gamma \propto 1/(\Lambda_1 - \langle \Gamma \rangle - \gamma)^{2-\alpha}$ . The behavior of the transmission coefficient is qualitatively similar to that of Lévy spatial diffusion coupled with a constant wave growth rate shown in Fig. 2. Similarly the mean energy density in the medium varies from the no-growth case shown in Fig. 3 asymptotically diverging and approaching the first pseudoeigenfunction in a qualitatively similar way to Fig. 5. For any given growth parameter  $(\langle \Gamma \rangle + \gamma)/\Gamma_{\text{las}}$ ,  $W(x)$  will have approached the first pseudoeigenfunction less closely than for the corresponding value of the growth parameter  $\Gamma/\Gamma_{\text{las}}$ , in the constant growth case.

For  $2 < \alpha < 3$ , the transmission coefficient rises from its no-growth case but does not diverge near the lasing threshold. The mean energy density also does not diverge near the lasing threshold and does not approach the first pseudoeigenfunction. This is similar to the wave modeled in Sec. IV B with Gaussian spatial scattering and a Lévy walk in gain which shows an increase in  $W(x)$  over the range of the parameter  $(\langle \Gamma \rangle + \gamma)/\Gamma_{\text{las}}$  but does not diverge and the shape  $W(x)$  changes only modestly compared to  $W(x)$  for  $1 < \alpha < 2$ .

## VI. SUMMARY AND CONCLUSIONS

We have studied random wave scattering and random wave growth using Lévy walks to model each case sep-

arately, in combination with Gaussian processes, or with both cases modeled with Lévy walks. Previous modeling of such processes using Gaussian statistics has been extended using a combination of analytic, numerical inversion and Monte Carlo techniques to systems where Gaussian statistics are not applicable.

The main results of this paper are as follows.

(i) For a system with Lévy spatial diffusion and a constant wave growth rate, transmission coefficients were obtained from a Laplace space method, bypassing the need for Monte Carlo simulations to obtain Lévy walk probability distributions. The use of operator shortcuts for obtaining properties allows both more efficient numerical computation and clearer qualitative understanding of the properties under investigation. As with Gaussian spatial diffusion subject to a constant wave growth rate, this system has a lasing threshold  $\Gamma_{\text{las}} = \Lambda_1$ . The transmission coefficient increases from its value in the absence of growth, diverging asymptotically as  $T_\Gamma \propto 1/(\Lambda_1 - \Gamma)$  near the lasing threshold.

(ii) For a system undergoing continuous injection with Lévy spatial diffusion and no wave growth, the mean energy density has been found. This smoothly varies with  $\alpha$  from the triangular form in the Gaussian case to the constant distribution as  $\alpha \rightarrow 1$ .

(iii) When a constant wave growth rate is added to the system in (ii) the mean energy density in the medium was obtained. As the wave growth rate varies, the mean energy density inside the medium varies from the no-growth case to asymptotically diverging near the lasing threshold. The mean energy density smoothly changes from the no-growth case to the first pseudoeigenfunction of the Lévy walk on a finite interval as the wave growth rate increases.

(iv) At some point below  $\alpha = 1.75$ , the concavity of the first pseudoeigenfunction reverses which was not described in our earlier work [7].

(v) A wave with a randomly varying wave growth rate where the variations in growth can be modeled as a Lévy walk in gain was analyzed in the absence of spatial scattering. The mean energy density of this wave  $\langle W(t) \rangle$  scales asymptotically at large times as  $\langle W(t) \rangle \sim (\gamma t)^{1-\alpha} e^{(\langle \Gamma \rangle + \gamma)t}$  for the entire range  $1 < \alpha < 3$ . This is in contrast with Gaussian diffusive random walks in gain, whose mean energy density remains exponential with redefined effective growth rates. A Gaussian walk based on the velocity model with a jump distribution with power law tail  $\alpha > 3$ , anomalously has a mean energy density with the same asymptotic functional form as Lévy walks. The exponential mean energy density of Gaussian diffusive random walks is only found for jump distributions with tails that fall more rapidly than any power law.

(vi) Gaussian spatial scattering is introduced to the wave undergoing random variations in its growth rate described by (v). For the entire range  $1 < \alpha < 3$  the lasing threshold is given by  $\langle \Gamma \rangle + \gamma = \lambda_1$  and is independent of the Lévy index  $\alpha$ . The mean energy density takes qualitatively different forms in each of the ranges  $1 < \alpha < 2$  and  $2 < \alpha < 3$ . For  $1 < \alpha < 2$  the mean energy density in the medium as a function of position varies from the triangular no growth case, asymptotically diverging near the lasing threshold and approaching

the first eigenfunction. This is qualitatively similar to the case of Gaussian spatial scattering coupled with a Gaussian random walk in gain. For  $2 < \alpha < 3$  the mean energy density does not diverge near the lasing threshold and does not asymptotically approach the first eigenfunction. Similarly the transmission coefficient for the system diverges near the lasing threshold for  $1 < \alpha < 2$  but not for  $2 < \alpha < 3$ .

(vii) Finally, Lévy spatial scattering is introduced to the wave undergoing random variations in its growth rate described by (v). The lasing threshold is given by  $\langle \Gamma \rangle + \gamma = \Lambda_1$  where  $\Lambda_1$  is the first pseudo-eigenvalue. The transmission coefficients and mean energy densities in the medium are qualitatively different in the two ranges of  $\alpha$ . For  $1 < \alpha < 2$  the transmission coefficient rises from the no-growth case diverging asymptotically as  $T_\Gamma \propto 1/(\Lambda_1 - \langle \Gamma \rangle - \gamma)^{2-\alpha}$  near the lasing threshold. The mean energy density in the medium varies from the no-growth case described in (ii) diverging near the lasing threshold and approaching the first pseudo-eigenfunction in a manner qualitatively similar to the waves described in (iii). For  $2 < \alpha < 3$  the transmission coefficient does not diverge as the lasing threshold is approached and the mean energy density in the medium neither diverges near the lasing threshold nor approaches the first pseudo-eigenfunction.

#### ACKNOWLEDGMENTS

This work was supported by the Australian Research Council.

#### APPENDIX: NOTE ON INCORRECT RESULT IN STANDARD INTEGRAL EQUATIONS HANDBOOK

In the relatively recently published and invaluable *Handbook of Integral Equations* [16] the authors have written and collated an encyclopedic collection of solution techniques and exact solutions to integral equations. In Eq. (21), p. 317, the handbook states

$$\phi(x) = \lambda \int_{-\pi}^{\pi} + K(x-t)\phi(t)dt, \quad (\text{A1})$$

for an even kernel  $K(x)=K(-x)$  for  $-\pi < x < \pi$ , can be solved with eigenfunctions  $\phi(x)=1$ ,  $\phi_n^{(1)} = \cos nx$ ,  $\phi_n^{(2)} = \sin nx$ . This is incorrect as can be shown by simply substituting the purported solutions into the integral equation. The result was collated from Kransov *et al.* [17] where the solution was justified by substitution back into the integral equation. Unfortunately this substitution was in error. An analytic solution to this class of integral equations would be of particular interest in the study of Lévy flights as these equations are connected with the eigenvalue equations of the turning point distributions. However, from the analysis in [7], which considers eigenvalues and eigenfunctions of the equation for the special class of kernels corresponding to those found in Lévy walk turning point equations, it is not anticipated a simple universal set of eigenfunctions exists for the broad range of kernel types which the tabulated result attempts to encompass.

- 
- [1] A. Ishimaru, *Wave Scattering and Propagation in Random Media* (Academic, New York, 1978).
  - [2] P. A. Robinson, *Philos. Mag. B* **80**, 2087 (2000).
  - [3] P. A. Robinson, *Phys. Rev. B* **55**, 12175 (1997).
  - [4] V. S. Letokhov, *Sov. Phys. JETP* **26**, 835 (1968).
  - [5] A. Davis and A. Marshak, in *Fractal Frontiers*, edited by M. Novak and T. G. Dewey (World Scientific, River Edge, NJ, 1997), p. 63.
  - [6] B. V. Gnedenko and A. N. Kolmogorov, *Limit Distributions for Sums of Independent Random Variables* (Addison-Wesley, Reading, MA, 1954).
  - [7] P. M. Drysdale and P. A. Robinson, *Phys. Rev. E* **58**, 5382 (1998).
  - [8] W. Feller, *Introduction to Probability Theory and its Applications* (Wiley, New York, 1974).
  - [9] H. Kesten, *Ill. J. Math.* **5**, 267 (1961).
  - [10] W. H. Press, S. A. Teukolsky, W. T. Vetterling, and B. P. Flannery *Numerical Recipes in Fortran*, 2nd ed. (Cambridge University Press, Cambridge, 1992).
  - [11] S. V. Buldyrev, S. Havlin, A. Ya. Kazakov, M. G. E. da Luz, E. P. Raposo, H. E. Stanley, and G. M. Viswanathan, *Phys. Rev. E* **64**, 41108 (2001).
  - [12] G. Zumofen and J. Klafter, *Phys. Rev. E* **47**, 851 (1993).
  - [13] G. Doetsch, *Introduction to the Theory and Application of the Laplace Transform* (Springer, Berlin, 1970).
  - [14] C. W. Gardiner *Handbook of Stochastic Methods*, 2nd ed. (Springer, Berlin, 1985).
  - [15] I. Podlubny, *Fractional Differential Equations* (Academic, London, 1999).
  - [16] A. D. Polyinin and A. V. Manzhirov, *Handbook of Integral Equations* (CRC Press, Boca Raton, FL, 1998).
  - [17] M. Krasnov, A. Kiselev, and G. Makarenko, *Problems and Exercises in Integral Equations* (Mir, Moscow, 1971).